Agriculture, Ecosystems and Environment 314 (2021) 107416

Contents lists available at ScienceDirect

Agriculture, Ecosystems and Environment

journal homepage: www.elsevier.com/locate/agee

Farming carbon: The link between saltwater intrusion and carbon storage in coastal agricultural fields

Elizabeth de la Reguera [a,b], Katherine L. Tully [a,*]

[a] Department of Plant Science and Landscape Architecture, University of Maryland, College Park, MD 20742, USA
[b] Department of Marine-Estuarine Environmental Science, University of Maryland, College Park, MD 20742, USA

ARTICLE INFO

Keywords:
Saltwater intrusion
Agriculture
Chesapeake Bay
Soil carbon
Soil aggregates
Wetland

ABSTRACT

As sea levels continue to rise, coastal agroecosystems have become more vulnerable to saltwater intrusion (SWI). Saltwater intrusion is the landward movement of sea salts, which can alter carbon (C) storage. Transitioning agricultural fields have the potential to become C sinks as SWI advances inland and turns farms to marshes. The objectives of our study were to (1) quantify the size of C pools along a salinity transect; (2) determine how soil C is occluded through levels of physical protection in soil aggregates; (3) examine relationships between indicators of SWI and soil C measures in coastal farm fields. We collected soils (to a depth of ~140 cm) along a transect from the edge of a salt-damaged field (high salinity and frequently inundated) to the center (low salinity and drier). We measured bulk soil C pools and the amount of C stored in large macroaggregates, small macroaggregates, microaggregates, and silt+clay size classes. Soil C pools were largest in the edge of field and ditch bank soils compared to the center of the field ($P = 0.01$). In ditch bank soils, most of the C was stored in large macroaggregates; however, in the center of the field, most C was stored in silt+clays. We suggest that frequent wetting events may lead to increased C storage along the edges of farm fields both as a result of suppressed decomposition rates and increased clay flocculation leading to macroaggregate formation. Further, a vegetation shift from annual, shallow-rooted crops to perennial, deeply rooted marsh grasses along field edges likely contributed to higher soil C levels as well as increased aggregation. An improved understanding of soil C dynamics can help inform management strategies that support farm and environmental wellbeing as our coastlines change.

1. Introduction

Coastal landscapes are on the forefront of climate change as global sea levels are projected to rise 0.5–1 m (1.8–3.2 ft) by 2100 (Church et al., 2013). A major consequence of sea level rise is saltwater intrusion (SWI), the landward movement of seawater. As 37% of the human population lives within 100 km of a coast (CIESEN SEDAC, 2020), SWI has the potential to impact coastal communities (e.g. plant, animal, and human) and agricultural systems across the world. For example, in Vietnam, SWI damages coastal rice paddies and sugarcane fields throughout the Mekong Delta, threatening the economy and local food security (Thanh, 2016; Gopalakrishnan et al., 2019). In the United States, both the east and west coasts are experiencing SWI from water withdrawal for agriculture and sea level rise (Barlow and Reichard, 2010; Wichelns and Qadir, 2015; Tully et al., 2019a).

Saltwater intrusion may also greatly alter the balance of carbon (C) additions and losses to soils. Soil organic matter (SOM) is the largest global reservoir of terrestrial organic C and plays an integral role in ecosystem function, soil fertility, and climate regulation (Paul et al., 2015). In the United States, agricultural soils are very low in soil C (~16 mg C g^{-1} soil from 0 to 40 cm; Martens et al., 2004) as compared to high-C soils in tidal wetlands (~150 mg C g^{-1} soil from 0 to 50 cm; Morris et al., 2016). Indeed, the practices of clearing for agriculture and tillage have released ~124 Pg of C to the atmosphere between 1850 and 1990 (Houghton and Hackler, 2008; Syswerda et al., 2011). However, SWI may create hotspots of C storage within farm fields as areas are exposed to variation in salinity, soil moisture, pH, and vegetation type, which may have an impact on aggregate formation and therefore C storage. This research investigates the potential for salt-intruded agricultural fields to become a C sink as SWI advances inland.

Until the late 20th century, the paradigm of soil organic C stabilization (maintaining C sequestration and storage in a given area) focused

* Corresponding author.
E-mail address: kltully@umd.edu (K.L. Tully).

https://doi.org/10.1016/j.agee.2021.107416
Received 30 October 2020; Received in revised form 23 February 2021; Accepted 16 March 2021
Available online 13 April 2021

on the importance of chemical recalcitrance (Schmidt et al., 2011; Dungait et al., 2012; Lehmann and Kleber, 2015). The theory proposed that recalcitrant compounds would decompose more slowly and thus were more stable compared to simple C compounds (Ågren and Bosatta, 2002; Dungait et al., 2012). However, subsequent systematic reviews have shown that C stabilization is also mediated by adsorption of C to clay minerals through cation bridging, the interaction of metal ions with organic matter, redox conditions, and the spatial inaccessibility of C inside soil aggregates (Jastrow et al., 2007; Sarkar et al., 2018; Sollins et al., 1996; von Lützow et al., 2007, 2006). Our research focuses on the spatial inaccessibility of C to microbial degradation. Soil C may be inaccessible to microbes and enzymes due to occlusion within aggregates at multiple levels of physical protection. The levels of physical protection are considered hierarchical (Six et al., 2000; Tisdall and Oades, 1982), suggesting that microaggregates (250–53 μm) are formed when silt+clay particles (< 53 μm) are bound by fungi, bacteria, and plant debris. Microaggregates are then bound together by plant-derived polysaccharides, roots, and fungal hyphae to form macroaggregates of varying size classes (> 250 μm; Six et al., 2000). The C associated with each aggregate size class becomes progressively more protected as smaller size classes are encapsulated inside larger aggregate size classes.

To date, the potential of agricultural fields undergoing SWI to accumulate and physically stabilize C via aggregation has not been investigated. However, there is a large body of research focused on the impacts of SWI on C in tidal freshwater wetlands indicating a range of responses. In freshwater wetlands, SWI can lead to increased organic C mineralization and thus accelerated soil organic C loss (Weston et al., 2006, 2011; Chambers et al., 2013). Other studies show the suppression of carbon dioxide (CO_2) emissions (suggesting C storage; Ardón et al., 2018; Herbert et al., 2018) in freshwater marshes exposed to salinity, perhaps as a result of microbial salt stress and overall declines in ecosystem productivity. Other research indicates that SWI into freshwater systems can decrease transport of dissolved organic C to coastal estuaries (Ardón et al., 2016) with consequences for detrital food webs and C cycling. The movement of saltwater onto agricultural landscapes occurs via hydrologically connected ditch networks and the groundwater table (Tully et al., 2019a). In the Mid-Atlantic (USA), the extensive agricultural ditch network was designed to drain excess water from farm fields, but is often serving the reverse purpose by acting as a conduit for saltwater to reach farm fields during high tides and storms (Bhattachan et al., 2018; Tully et al., 2019a). As saltwater moves onto agricultural fields, soils closest to agricultural ditches experience frequent wetting with high salinity water, while soils further inland (center of fields) do not experience frequent wetting. Frequent soil wetting creates anaerobic conditions, which may slow decomposition rates of soil organic C compared to aerobic soils, resulting in increased C storage (Bridgham et al., 2006; Mitsch and Gosselink, 2015). We hypothesize soils closest to the saltwater source (near agricultural ditch) will store more C than soils in the center of agricultural fields because of slower decomposition rates and suppressed CO_2 emissions as soils are wetter and saltier. Our work is the first study to investigate the potential of agricultural soils to store C as they undergo SWI and, more specifically, the degree to which that C is protected and stabilized.

The main objectives of this study were to: (1) quantify the size of soil C pools along a SWI gradient in coastal farm fields; (2) determine how soil C is occluded through levels of physical protection; (3) examine relationships between indicators of SWI and soil C measures in coastal farm fields. We established transects on six agricultural fields on the Lower Eastern Shore of Maryland that spanned a SWI gradient from the ditch bank (salty and frequently inundated) to the center of the agricultural field (fresh and drier). We hypothesize that larger soil C pools in soils closest to the saltwater source (e.g. ditch bank). Further, we hypothesize that the soil C would be associated with large macroaggregates in ditch bank soils, and that changes in C would be related to variations in soil moisture and salinity across the transect.

2. Methods

2.1. Study sites

Our study sites are located on the Lower Eastern Shore of the Chesapeake Bay in Maryland (Fig. 1). Salinity is high in the mouth of the Chesapeake Bay (~25 ppt) and declines northward; salinity in monitoring stations close to our study region in March 2018 ranged from 10.2 to 12.5 ppt (Chesapeake Bay Program, 2021). Sea level rise rates in the region have increased from ~1–3 mm per year in the 1930s to ~4–10 mm year in 2011 (Ezer and Corlett, 2012). The mean elevation of our study sites is 1 m above sea level (Table 1), and it is estimated that sea levels will rise by 0.3–0.6 m (0.9–2.1 ft) by 2050 (Boesch et al., 2013), making coastal farms in the Chesapeake Bay highly vulnerable to saltwater intrusion.

From the mid 1600s to the early 1700s, the region was heavily forested with a small portion of the land (~5%) in low-intensity tobacco and corn cultivation that included long (~20 year), regenerative fallow periods (Benitez and Fisher, 2004). However, by 1800, ~80% of the land was converted to agriculture (tobacco and wheat) with shorter fallows (~2 year) and little primary forest remained (Benitez and Fisher, 2004). Indeed, many farm fields in our study region have been cultivated for the last 400 years. The typical crop rotation in the region is corn (*Zea mays*)-soybean (*Glycene max*)-wheat (*Triticum aestivum*), and no-till techniques have been utilized for the last 40 years (Huggins and Reganold, 2008). We selected five actively managed salt-intruded farm fields in Somerset Co. and one in Dorchester Co., Maryland on which to conduct this study (Table 1; Table S1; Appendix A). The majority of soils in Somerset Co. are Quindocqua silt loams with little to no slope and in Dorchester Co. are frequently flooded Honga peat (USDANRCS, 2020; Fig. S1). Study sites are located within 540 m of tidal creeks, and we observe daily fluctuations of 6 cm in groundwater levels (daily max recorded = 44 cm), a signature of diurnal tidal variation (Jones, unpublished data). The effects of SWI on soil chemical changes were described in detail for three of the farms by Tully et al. (2019b).

Farms 1, 2, 4, 5, and 6 are predominantly silt loam soils, while Farm 3 is predominantly a sandy loam soil (USDANRCS, 2020; Table 1; Fig. S1). Preliminary studies show that soils are fairly acidic, and that soil pH does not vary strongly by depth or across the intrusion transect (pH range of 4.6–6.3). All six farms show evidence of SWI, with saltier soil near the agricultural ditch (~10 ppt). Towards the center of the fields, each farm has a relatively healthy crop stand and low soil salinity (~1 ppt). The intrusion area is characterized by five distinct zones: ditch bank, field edge, bare, crop edge, and crop (Tully et al., 2019b). Ditch banks tend to be dominated by *Phragmites australis* (invasive reed species). Field edges contain a mixture of herbaceous marsh species (e.g. *Aster subulatus*, *Spartina patens*) and agricultural weeds (e.g. *Erigeron canadensis* and *Sorghum halepense*). The bare zone separates the field edge and crop edge and is characterized by a complete lack of plant growth, cracked soil, and visible salt deposits. Incomplete crop germination or stunted plants pepper the crop edge zone. The crop zone has evenly spaced, healthy crop plants. As farms in this region are rapidly converting to tidal marshes (Gedan et al., 2020), these transects can be considered a space-for-time substitution with which we can evaluate the effect of SWI on soil C dynamics as a farm converts to a wetland. At each farm, we identified a SWI transect, which ranged from 26 to 78 m long across each field (Table 1) the fall prior to soil collection. All five zones were sampled from Farms 3, 4, and 5. In Farms 1, 2, and 6, only four zones were sampled due to impenetrable vegetation and unstable soils along the ditch banks.

2.2. Soil collections

We collected soil samples in early-March 2018 before cash crops were planted and following a winter fallow/cover crop in all cases. We collected soils early in the season as both plant and microbial activity

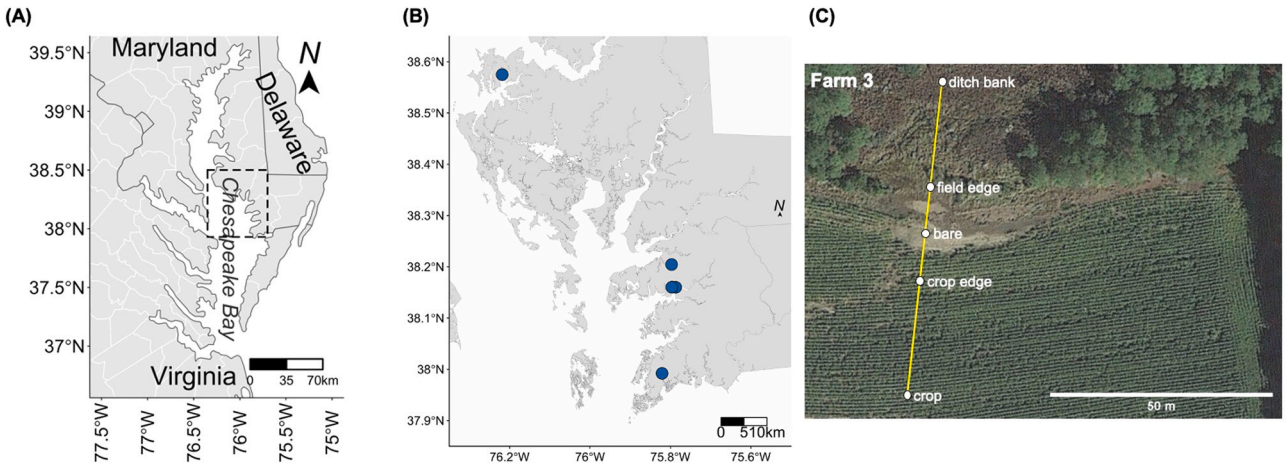

Fig. 1. (A) Map of the Chesapeake Bay region, United States. Study area is outlined by the dotted rectangle; (B) map of the study area and agroecosystem site locations (blue dots) in Somerset County and Dorchester County, Maryland; (C) satellite imagery of one of the study sites with labeled transect points along the intrusion zone. Panel C imagery taken from Google Earth (Google Earth, 2020).

Table 1
Characteristics of the six no-till focal farms on the Eastern Shore of Maryland.

	Farm 1	Farm 2	Farm 3	Farm 4	Farm 5	Farm 6
County	Somerset	Somerset	Somerset	Somerset	Somerset	Dorchester
Previous crop rotation (2017)	Corn-soybean	Soybean-winter rye cover crop	Sorghum	Fallow	Fallow	Sorghum
Texture class	Silt loam	Silt loam	Sandy loam	Silt loam	Silt loam	Silt loam
Soil type	Mesic Typic Hapludults	Mesic Typic Hapludults	Mesic Typic Endoaquults	Mesic Typic Endoaquults	Mesic Typic Endoaquults	Mesic Typic Endoaquults
Soil series	Queponco	Queponco	Othello-Fallsington complex	Quindocqua	Quindocqua	Elkton
Length of transect (m)	56	78	71	34	26	27
Elevation (m)	2	1	1	2	2	1

were suppressed at this point, allowing us to control for the effect of actively growing vegetation on SOC pools. Soils were collected to ~140 cm with a 7-cm diameter bucket auger in each field at each zone along the intrusion transect. Soil horizons were described in the field and compared to the series mapped by Web Soil Survey (USDA NRCS, 2020). Then, soil samples were homogenized by horizon, which were visually distinct across the transect. Separating soils by horizon rather than a prescribed depth allowed us to maintain standard protocols across the entire transect. A sub-sample (~200 g) of the homogenized soil was used for aggregate size separation. An additional subset was weighed wet, oven-dried at 105 °C for 48 h and then reweighed to determine gravimetric soil moisture content. The remaining soil (herein referred to as "bulk soil") was sieved through a 4.75 mm mesh and air-dried.

Initial tests confirmed that there was no inorganic C present, and thus air-dried soils were analyzed for %C using dry combustion (LECO TruMac N, St. Joseph, MI). Soil bulk density cores were collected along the intrusion transect every 10 cm in the top 50 cm and dried at 105 °C for 7 days. For bulk density values below 50 cm, we used a bulk density estimate from the Web Soil Survey based on the soil series type and horizon for that sample (USDA NRCS, 2020). We confirmed horizon structure in the field to Web Soil Survey and then calculated a weighted average of bulk density for each horizon depth of interest.

2.3. Bulk soil C metric

Because cores varied in depth along the transect and among farms, we used a consistent soil depth of 100 cm to calculate bulk total soil C pool (Mg C ha^{-1}), which was calculated by multiplying the C concentration of bulk soil (mg C g^{-1}; Fig. S2) by the bulk density (g cm^{-3}), and the soil depth segment (cm; Table S2; Eq. (1)). These values were summed for all segments up to 100 cm.

$$Bulk\,C\,pool = \Sigma(C\,concentration * bulk\,density * depth\,segment * 100) \quad (1)$$

2.4. Aggregate size and C metrics

The 200 g sub-sample of soil was passed through a 4.75 mm sieve and a 100 g sub-sample was fractionated into five size classes using the slaking method developed by Six et al. (2000). All aggregate sizes were force air-dried in an oven at ~65 °C for at least 4 days. Rocks larger than 250 μm were removed from the large and small macroaggregates. Large macroaggregates, small macroaggregates, and microaggregates were measured for sand content using the pipette method to avoid over-estimating C pools (see Appendix B), as sand is not defined as an aggregate (Six et al., 2000). Soils (without rocks) were ground for %C using dry combustion.

To determine the sand-free aggregate mass (g), the sand mass (g) was subtracted from the total aggregate mass (g; Table S2; Eq. (2)).

$$Sand\ free\ aggregate\ mass = total\ aggregate\ mass - sand\ mass \quad (2)$$

In order to determine the proportion of each aggregate size class within a soil sample, we calculated the aggregate distribution (g aggregate g^{-1} soil) by dividing the sand-free aggregate mass (g) by the sum of the sand-free aggregate mass of the soil sample (g; Fig. S3; Eq. (3)).

$$Agg\ distribution = \frac{sand\ free\ aggregate\ mass}{\Sigma(sand\ free\ aggregate\ mass\ of\ soil\ sample)} \quad (3)$$

We calculated total aggregate C of sand-free aggregates (g C) by

multiplying C concentration (mg C g^{-1}) by sand-free aggregate mass (g) and then dividing by 1000 (conversion factor; Eq. (4)).

$$Total\ aggregate\ C = \frac{C\ concentration * sand\ free\ aggregate\ mass}{1000} \quad (4)$$

In order to determine the proportion of aggregate C within soil, we calculated the normalized total aggregate C (g C g^{-1} C) by dividing the total aggregate C of sand-free aggregates (g C) by the sum of the total aggregate C of the large macroaggregates, small macroaggregates, microaggregates, and silt+clay in a given sample (Eq. (5)).

$$Norm\ agg\ C = \frac{Total\ aggregate\ C}{\Sigma\ (total\ aggregate\ C\ of\ LM,\ sM,\ m, sc\ in\ a\ given\ \ \ sample)} \quad (5)$$

Where, LM stands for large macroaggregate, sM stands for small macroaggregate, m stands for microaggregate, and sc stands for silt+clay.

2.5. Indicators of saltwater intrusion

In order to examine the effects of SWI on soil C, we examined a suite of proxy drivers: soil pH (cation bridging), electrical conductivity (salinity), and changes in wetness (soil moisture). Soil EC and pH were measured using a conductivity probe and pH probe attached to a multiparameter benchtop meter (Orion Versa Star Pro, Thermo Fisher Scientific, Hampton, NH, USA). As previously mentioned (Section 2.2), we measured gravimetric soil moisture content in all bulk soils and used this as our proxy for field wetness. We acknowledge that gravimetric soil moisture only allows for a "snapshot" of field conditions at the time of soil collection. Ideally, we would have installed redox probes or IRIS films (Rabenhorst, 2008) to measure fluctuations in redox conditions along the SWI transect. However, as all of the sites selected were located on working agricultural fields, farmers expressed concerns about permanent equipment installations. Further, pilot experiments resulted in the destruction of instrumentation by farming equipment. Thus, we decided to use gravimetric soil moisture, a more crude, but consistent measurement for soil wetness in this study.

2.6. Statistical analysis

First, we tested the effect of soil depth on soil C concentration (mg C g^{-1}) in bulk soils because bulk soil C pools and aggregate C are subsets of (or calculated from) the bulk soil C concentration. Based on these preliminary tests, we grouped soil horizons into four categories of increasing depth: 0–20 cm, ~20–50 cm, ~50–80 cm, and ~80+ cm.

Upon initial inspection, we found that soil C concentrations were most variable across the transects in the upper 20 cm of soil. Therefore, we examined the relationship between soil C concentration and indicators of SWI (EC, pH, and soil moisture) in the topsoil (0–20 cm) across the whole transect (all points included) and at each point along the transect using Pearson correlations. Given the number of comparisons generated for each soil variable (n = 6), a Bonferroni-corrected α ($P < 0.008$) was used to reduce Type I error. We did not observe strong relationships between continuous soil variables and soil C indicating that using a point measurement of soil EC, pH, or soil moisture fails to accurately represented the long-term effects of SWI. Thus, we used the categorical variable of transect point to represent the sustained effects of SWI on soil C.

To examine the effect of SWI on total bulk soil C pools (to 100 cm), we ran linear mixed-effects (LME) models (*lme4* package for R; Bates et al., 2015) with transect point (i.e. crop, crop edge, bare, field edge, and ditch bank) as the main effect and farm as a random effect (Table S3). In addition, we examined the size of the bulk C pools at the four depth categories to determine if different soil depths were more sensitive to the effects of SWI. Therefore, we used a similar LME model with transect as the main effect and farm as a random effect to look at changes in soil C pools across the transect for each depth category separately (total of four LME models: 0–20, ~20–50, ~50–80, ~80+ cm; Table S4). We used Tukey post hoc tests using the *multcomp* package in R (Hothorn et al., 2008) to examine the effect of transect location on soil C pool size. Significance was determined at $P < 0.05$.

As with bulk soil C concentrations, we examined the relationships between total aggregate C at each size class and indicators of SWI (EC, pH, and soil moisture; 0–20 cm) at each point along the transect using Pearson correlations. Given a large number of comparisons generated (n = 20), a Bonferroni-corrected α ($P < 0.0025$) was used to reduce Type I error. Similar to bulk soil C concentrations, a lack of strong relationships between continuous soil variables and total aggregate C led us to use categorical variable of transect point to represent the sustained effects of SWI.

To determine if total aggregate C (g C) is stored in different size classes (a measure of physical protection) along a SWI transect, we used four LME models (one for each depth category) with transect point and aggregate size class as main effects and farm as a random effect (Tables S5–S12). In each case, we used Tukey post hoc tests to examine differences in aggregate size class or location on the SWI transect using the *multcomp* package in R. Significance was determined at $P < 0.05$.

When necessary, we used Box-Cox transformations (Box and Cox, 1964) prior to analysis to satisfy the assumptions of the statistical models. Statistical analyses were conducted in the R environment for Macintosh (v1.2.1335; R Core Team, 2019).

3. Results

3.1. Ditch bank soils have the largest bulk soil C pool

As soil C pool size would differ by the size of the depth segment (e.g. 10 cm segment is smaller than a 30 cm segment), we analyzed depth categories separately. We found significantly larger soil C pools in the ditch bank soils than all other locations on the transect in the 0–20 cm and ~20–50 cm depth categories ($P = 0.04$ in both cases; Fig. 2). Soil C pools in field edge soils (19.7 Mg C ha^{-1}) were 1.2 times larger than the crop, crop edge, and bare soils at 0–20 cm (16.1 Mg C ha^{-1} on average) and 2 times larger at ~20–50 cm depth categories (22 Mg C ha^{-1} compared to 11.5 Mg C ha^{-1} on average), but still smaller than the ditch bank soil C pools. In deep soils (~50–80 and 80+ cm), we observed no effect of transect location on bulk total C pools.

Total bulk soil C pools (0–100 cm) varied significantly across the SWI transect ($P = 0.009$), and trends were driven by the patterns observed in the upper two depth categories (0–20 cm and ~20–50 cm). Overall, soil C pools were highest in ditch bank soils (85.9 Mg C ha^{-1}) and lowest in crop soils (36.5 Mg C ha^{-1}). Total bulk C pools in field edge soils (48.1 Mg C ha^{-1}) were 1.5 times larger in the crop, crop edge, and bare soils (36.2 Mg C ha^{-1} on average), but still ~2 times smaller than the ditch bank soil C pools (Fig. 2).

3.2. Soil C is stored in different aggregate size classes across a SWI transect

Because soil C concentrations varied significantly across the transect with depth category (0–20 cm, ~20–50 cm, ~50–80 cm, ~80+ cm), we examined the effect of transect location and aggregate size class at each depth category separately. In the 0–20 cm depth category, the large macroaggregates contained the lowest total aggregate C (g C) at the crop, crop edge, and bare locations, but the highest aggregate C at the field edge and ditch bank locations (compared to microaggregates and silt+clays; Fig. 3A). At 0–20 cm, aggregate C in the large and small macroaggregate size classes comprised 65% of the total aggregate C in the field edge soils and 70% of the total aggregate C in ditch bank soils (Fig. S4A).

In the ~20–50 cm depth category, there was a significant interaction

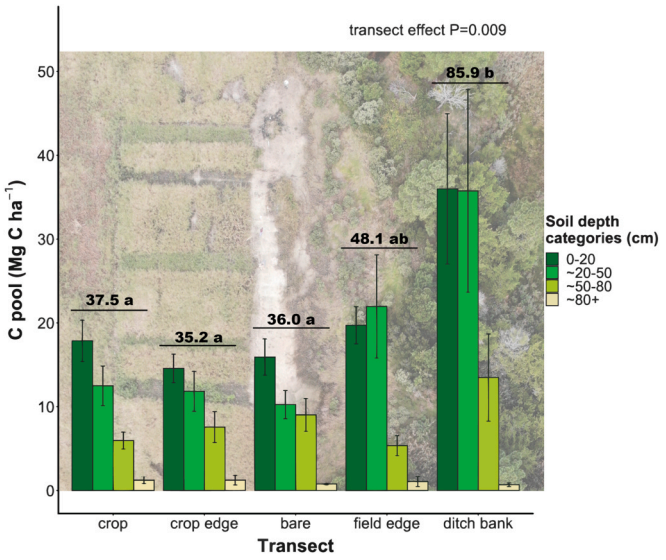

Fig. 2. Bulk soil C pool (Mg C ha^{-1}) in bulk soils (not fractionated by size class) along the SWI transect at 0–20 cm, ~20–50 cm, ~50–80 cm, and ~80+ cm. Error bars are the standard error of the mean. Values above horizontal bars indicate the size of the total bulk soil C pool for each transect location. Different letters are statistically significant at $P < 0.05$ in Tukey post hoc pairwise comparison. Background image is an aerial photograph of a transect.

between location on the transect and aggregate size class on total aggregate C at the ~20–50 cm soil depth ($P = 0.04$). This pattern was driven by changes in the large macroaggregate size class alone, whereby large macroaggregates had the lowest total aggregate C at the crop, crop edge, and bare locations, but in the field edge and ditch bank soils, macroaggregates held an equal amount of total aggregate C to all other size classes in the field edge and ditch bank soils (Fig. 3B). Aggregate C of large and small macroaggregates comprised ~55% of the total aggregate C found in the field edge soils and ~45% in the ditch bank soils at ~20–50 cm (Fig. S4B).

In soils from ~50–80 cm and ~80+ cm, there was no significant interaction between the location on the transect and aggregate size class and no effect of transect location alone on total aggregate C. There was a significant effect of size class on total aggregate C ($P < 0.0001$) at both ~50–80 and ~80+ cm, whereby the total aggregate C of silt+clays was significantly greater compared to small macroaggregates at all five transect locations ($P = 0.001$; Fig. 3C, D). Total aggregate C in silt+clay size class comprised 45% of the total aggregate C found in crop, crop edge, bare, field edge, and ditch bank soils at ~50–80 cm and at the deepest soils (Fig. S4C, D).

3.3. Soil C levels increase with soil moisture in wet parts of the field

Across the fields, in the top 20 cm of soil, we found positive correlations between soil C concentration and EC ($r = 0.60$, $P < 0.0001$; Fig. S5). However, we did not observe significant correlations (at $\alpha < 0.008$) between EC and soil C concentrations (0–20 cm) at any of the zones along the SWI transect. We found an overall increase in soil C concentrations with soil moisture ($r = 0.88$, $P < 0.0001$; Fig. S6), driven by multiple zones on the SWI transect. Soil C concentrations at the field edge ($r = 0.85$, $P = 0.0009$) and ditch bank ($r = 0.97$, $P = 0.002$) zones showed a strong positive correlation with soil moisture (Fig. 4D, E). There was no correlation between soil C concentration and pH (a proxy for cation bridging) at any location on the SWI transect.

When examining relationships between total aggregate C for each size class and indicators of SWI, we observed a strong positive correlation between soil moisture and the total aggregate C of large macroaggregates, small macroaggregates, and microaggregates at the ditch bank zone ($r = 0.99$ in all cases, $P < 0.002$ in all cases; Fig. 5E, J, and O). There was also a strong positive correlation between soil moisture and the small macroaggregates at the field edge ($r = 0.84$, $P = 0.002$; Fig. 5I). We found no significant relationships between the total aggregate C of silt+clay and soil moisture along the intrusion transect. There were no significant relationships between soil EC or pH at any point along the transect and total aggregate C in any of the size classes.

4. Discussion

This study is the first to explore the effects of SWI on soil C in agricultural soils by (1) quantifying the size of C pools along a SWI transect; (2) understanding how soil C is protected within aggregate size classes; (3) examining relationships between indicators of SWI and measures of soil C. Overall, we found larger soil C pools (and higher bulk C concentrations) in the ditch banks than in the center of salt-intruded fields. We also observed large amounts of total aggregate C in large and small macroaggregates in the ditch bank soils in the top 50 cm of the soil profile, suggesting that C in these soils is likely physically protected from microbial degradation. Finally, we found that one-time measurements of soil EC, moisture, and pH were not strongly correlated to soil C measures. However, among these variables, measures of soil C increased most strongly with soil moisture.

4.1. Moisture and salinity effects on soil C

We observed the largest soil C pools in soils on the edges and ditch banks of salt-intruded farm fields (Fig. 2), likely due to the combined effect of SWI on abiotic and biotic factors (e.g. moisture levels and vegetation). For example, frequent soil wetting creates anaerobic conditions, which may slow decomposition rates of soil organic C compared to aerobic soils, resulting in increased C storage (Bridgham et al., 2006; Mitsch and Gosselink, 2015). Offering further support, we observed an overall strong positive relationship between soil moisture and topsoil C concentrations (Fig. S6). Wetting events can also dissolve strongly-crystalline iron oxides into poorly crystalline structures under anoxic conditions (Wahid and Kamalam, 1993; Hall et al., 2018); Tully et al. (2019b) showed the structure of Fe changed from strongly crystalline to poorly crystalline along a SWI transect on coastal agricultural fields (Farms 1, 2, and 3 in this study). We were unable to either directly (Eh probes) or indirectly measure soil redox (IRIS films; Rabenhorst, 2008) as the fields were still under active management. However, future studies should attempt to locate recently abandoned agricultural fields to determine the effect of SWI on redox condition and its consequences for soil C storage.

We observed the highest amounts of total aggregate C in the ditch banks zones (primarily stored in macroaggregates), likely due to the influence of fluctuating moisture conditions. Wetting events can lead to increased soil aggregation depending upon clay mineralogy (Singer et al., 1992; Attou et al.,1998; Bronick and Lal, 2005). In soils containing non-swelling clays (e.g. kaolinite), clay particles will disperse when wet but form clay bridges and coatings among silt particles as they dry, thus supporting flocculation and aggregation (Attou et al.,1998). Focal fields contain primarily kaolinitic clays (Wilson, 1999), suggesting the soils tend to disperse when wet but aggregate as they dry (Weil and Brady, 2016). Thus, aggregation in the ditch bank soils was partially explained by clay dispersion and flocculation following repeated wetting events.

The edges of farm fields and ditch banks had a higher salinity (~7 ppt) than the center of the fields (3 ppt; Tully et al., 2019b), and we observed an overall increase in topsoil C concentrations with EC (Fig. S5), however this trend was not significant when we looked at individual transect points. This is likely because a point measurement of soil salinity is a poor predictor of soil C levels. Soil C can decline or accumulate on the order of years or decades (Grandy and Robertson, 2007; Stockmann et al., 2013) and soil salinity can fluctuate on much shorter timescales in response to freshwater availability (Tully,

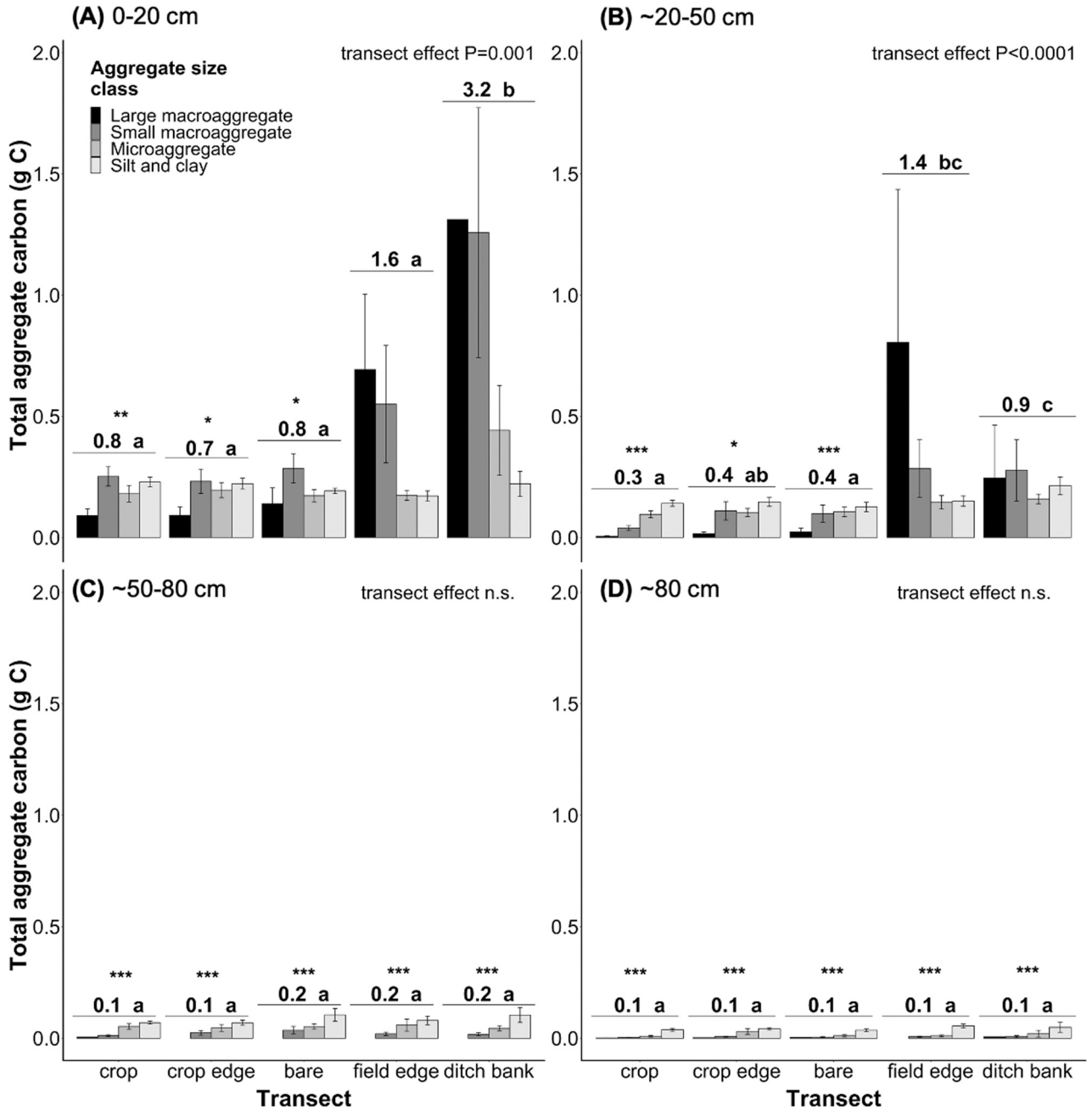

Fig. 3. Total aggregate C (g C sand-free aggregate) in (A) 0–20 cm, (B) ~20–50 cm, (C) ~50–80 cm, and (D) ~80+ cm along the SWI transect. Error bars are the standard error of the mean. Values above horizontal bars indicate the total aggregate C for each transect location. Different letters are statistically significant at $P < 0.05$ in Tukey post hoc pairwise comparisons. Asterisk (*) indicates significance by class within a transect point at *$P < 0.05$, **$P < 0.01$, ***$P < 0.005$ in Tukey post hoc pairwise comparisons.

unpublished data). Thus, future work should track soil C and salinity over multiple years to capture the long-term effect of fluctuations in soil salinity on C pools. Finally, although we expected soil C concentrations might increase with pH due to its influence on cation bridging, we saw no significant trends despite a rather large range of soil pH (4.3–6.3, Table S1), but as the soils are fairly acidic, it is likely that cation bridging may not exert a strong control on soil C in the focal farms.

4.2. Vegetation effects of SWI on soil C

In addition to abiotic drivers, the pattern in C pools and aggregate-associated C can also be explained by biotic factors such as changes in vegetation type, structure, and management. The center of the farm field is dominated by a monoculture agricultural crop (e.g. corn, soybean, sorghum), the crop edge is characterized by patchy, poorly performing crop, and the bare area has no vegetation. Although the field edge is still actively managed (e.g. planted, sprayed with herbicides, mowed), crops are unable to grow. As farm fields transition into wetlands, annual weed abundance (e.g. *Erigeron canadensis, Sorghum halpense, and Setaria faberi*) tends to decline, and they become increasingly dominated by native, perennial, and wetland species (Gedan and Fernández-Pascual, 2019). The edges of salt-damaged fields in the region are populated by salt-tolerant annual native forbs like *Aster subulatus* and *Solidago sempervirens* as well as perennial wetland grasses like *Spartina patens* and *Distichlis spicata* (Gedan and Fernández-Pascual, 2019). Wetland grasses species, which have deeper rooting systems (15–51 cm; USDA NRCS,

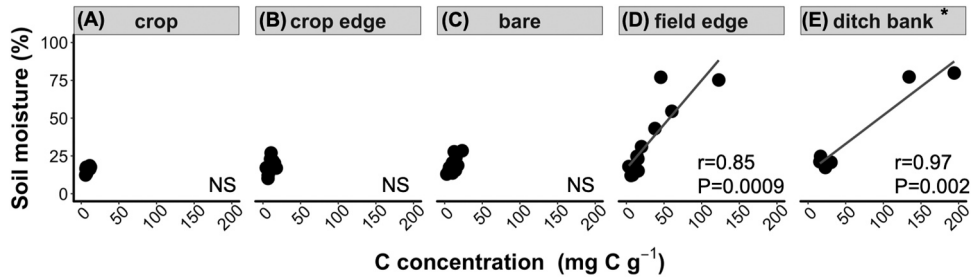

Fig. 4. Correlation between soil C concentration (mg C g^{-1}) and soil moisture (%) from 0 to 20 cm across all sites (Farms 1–6) at transect points (A) crop, (B) crop edge, (C) bare, (D) field edge, and (E) ditch bank. Asterisk (*) indicates fewer samples at the ditch bank zone compared to other zones on the intrusion transect because only Farms 3, 4, and 5 were sampled in the ditch bank.

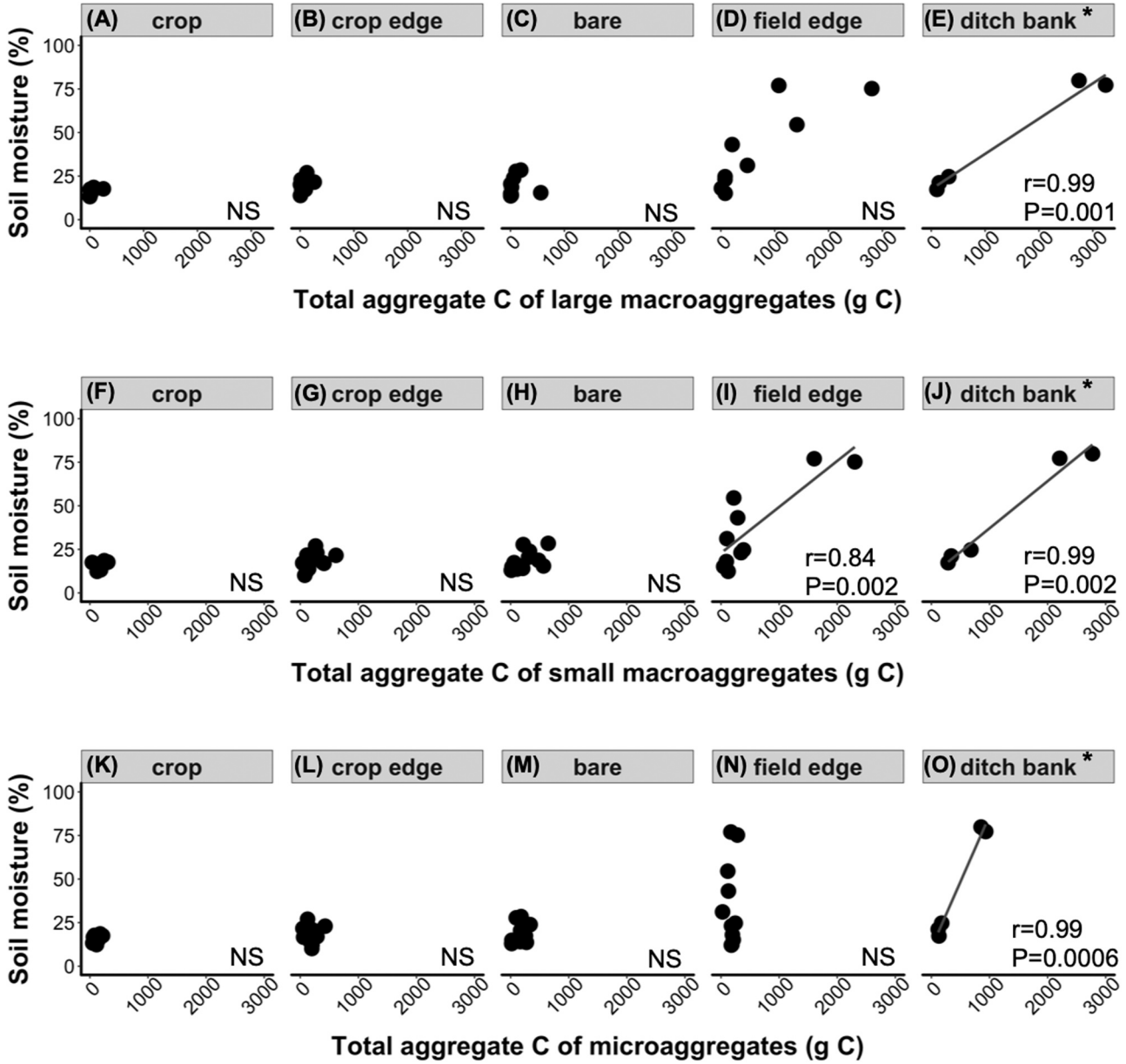

Fig. 5. Correlation between total aggregate C (g C) of large macroaggregates and soil moisture (%) from 0 to 20 cm across all sites (Farms 1–6) at transect points (A) crop, (B) crop edge, (C) bare, (D) field edge, and (E) ditch bank; total aggregate C (g C) of small macroaggregates and soil moisture at (F) crop, (G) crop edge, (H) bare, (I) field edge, and (J) ditch bank; total aggregate C (g C) of microaggregates and soil moisture at (K) crop, (L) crop edge, (M) bare, (N) field edge, and (O) ditch bank. Asterisk (*) indicates fewer samples at the ditch bank zone compared to other zones on the intrusion transect because only Farms 3, 4, and 5 were sampled in the ditch bank.

2017) than standard annual crops (10–20 cm; Fan et al., 2016), may trap sediments and their associated organic C, thereby increasing soil C pools (Mcleod et al., 2011; Kell, 2012). Root depth distribution is one of the most important plant traits controlling root soil C storage (Poirier et al., 2018; Sanaullah et al., 2010; Lorenz and Lal, 2005) and stabilization due to its influence on rhizodeposition (von Lützow et al., 2006; Jones et al., 2009), root chemistry (Cotrufo et al., 2013, 2015), and sphere of influence on soil minerals and metals (Feng and Simpson, 2007; Poirier et al., 2018; von Lützow et al., 2006; Watteau et al., 2006). For example, roots release exudates that are primary precursors of SOM formation as microbes utilize exudates efficiently, they are rapidly converted to secondary products and biomass, which can be stabilized by soil minerals (Bradford et al., 2013; Cotrufo et al., 2013; Lehmann and Kleber, 2015). In addition, root-associated symbionts play a key role in SOC accumulation as they enmesh soil particles and release organic compounds that hold microaggregates together, thus forming highly stable macroaggregates that store more C than smaller size classes (Bronick and Lal, 2005; Drury et al., 1991; Grandy and Robertson, 2007; Perfect et al., 1990; Six et al., 2000; Tisdall and Oades, 1982). Therefore, the type, structure, and management of vegetation (e.g. mowing, spraying herbicide) at the field edge and ditch banks may alter the accumulation of soil C and thus, the amount of C associated with large macroaggregates. Future research should investigate how shifts in vegetation (and specifically roots) may alter C dynamics as farmlands transition to wetlands.

4.3. *From farmland to wetland*

Sea levels continue to rise across the globe, pushing SWI further inland. Our agricultural systems are on the front-lines of climate change, and studies like this are critical for understanding (1) how they are going to respond and (2) if we can better manage them as they transition. That is, as SWI continues to move inland and onto agricultural fields, we may be able to manage these fields in such a way that they can store more C (through physical protection in soil aggregates). The focal farm fields have been experiencing SWI for at least a century, but the effects have worsened within the last five decades (Larry Fykes, *personal communication*; Gedan et al., 2020). Understanding and quantifying the change in soil C pools and how C is protected in soils in fields experiencing SWI is crucial as they have the potential to become C sinks and, ultimately, "blue carbon" ecosystems. Blue C ecosystems (e.g. mangroves, tidal wetlands, seagrass meadows) are highly efficient C sinks because the soil does not become saturated with C due to vertical accretion and dense vegetation with complex rooting systems (Chmura et al., 2003; Mcleod et al., 2011). Here, we show that soils on the edges of transitioning agricultural fields have the potential to sequester and store C at the same scale as blue C ecosystems. It is estimated that between 10% and 23% of agriculture in coastal countries such as Vietnam, Egypt, and Bangladesh are vulnerable to sea level rise (and likely SWI; Chen et al., 2012), perhaps we should consider practices that allow us to "farm" C in some coastal agricultural areas.

In the US, there exist state- and federally-funded conservation programs that pay farmers to take marginal land out production and establish buffers or wetlands, thus altering the vegetation type and structure with the potential to store more C (e.g. Conservation Reserve Program, Environmental Quality Incentives Program). In addition, wetland restoration projects may receive C credits on the voluntary C market if the project increases C sequestration and/or reduces C emissions. Understanding the abiotic and biotic factors that drive C sequestration in coastal agricultural fields will help inform best management practices for coastal resiliency (MDP, 2019).

5. Conclusion

This is the first study to our knowledge that has quantified soil C pools and the degree to which soil C is physically protected in aggregates along a SWI transect in coastal farm fields. Overall, we found the largest soil C pools in the ditch bank soils compared to all other locations on the SWI transect. Additionally, most of the C was stored in the top 50 cm and in the large macroaggregate size class in the ditch bank soils. Finally, measures of soil C increased most strongly with soil moisture compared to soil EC and pH. Farmlands experiencing SWI are at the forefront of climate change and rising sea levels. The management of these lands is crucial if we want to preserve soil C now and sequester more C in the future.

Declaration of Competing Interest

The authors declare that they have no known competing financial interests or personal relationships that could have appeared to influence the work reported in this paper.

Acknowledgements

This research was supported by the United States Department of Agriculture - National Institute for Food and Agriculture (Grant no. 12451226) project accession no. 1015143, a grant from the Harry R. Hughes Center for Agro-Ecology, and the National Socio-Environmental Synthesis Center (Grant no. DBI-1639145). We would like to thank the farmers and landowners of Somerset and Dorchester County, Maryland, who allowed research to be conducted on their salt-intruded farm fields. The authors claim no conflict of interest.

Appendix A. Supporting information

Supplementary data associated with this article can be found in the online version at doi:10.1016/j.agee.2021.107416.

References

Ågren, G.I., Bosatta, E., 2002. Reconciling differences in predictions of temperature response of soil organic matter. Soil Biol. Biochem. 34, 129–132. https://doi.org/10.1016/S0038-0717(01)00156-0.

Ardón, M., Helton, A.M., Bernhardt, E.S., 2016. Drought and saltwater incursion synergistically reduce dissolved organic carbon export from coastal freshwater wetlands. Biogeochemistry 127, 411–426. https://doi.org/10.1007/s10533-016-0189-5.

Ardón, M., Helton, A.M., Bernhardt, E.S., 2018. Salinity effects on greenhouse gas emissions from wetland soils are contingent upon hydrologic setting: a microcosm experiment. Biogeochemistry 140, 217–232. https://doi.org/10.1007/s10533-018-0486-2.

Attou, F., Bruand, A., Le Bissonnais, Y., 1998. Effect of clay content and silt-clay fabric on stability of artificial aggregates. Eur. J. Soil Sci. 49, 569–577.

Barlow, P.M., Reichard, E.G., 2010. Saltwater intrusion in coastal regions of North America. Hydrogeol. J. 18, 247–260. https://doi.org/10.1007/s10040-009-0514-3.

Bates, D., Mächler, M., Bolker, B., Walker, S., 2015. Fitting linear mixed-effects models using lme4. J. Stat. Softw. 67 https://doi.org/10.18637/jss.v067.i01.

Benitez, J.A., Fisher, T.R., 2004. Historical land-cover conversion (1665-1820) in the Choptank Watershed, Eastern United States. Ecosystems 7. https://doi.org/10.1007/s10021-003-0228-0.

Bhattachan, A., Emanuel, R.E., Ardon, M., Bernhardt, E.S., Anderson, S.M., Stillwagon, M.G., Ury, E.A., Bendor, T.K., Wright, J.P., 2018. Evaluating the effects of land-use change and future climate change on vulnerability of coastal landscapes to saltwater intrusion. Elem. Sci. Anthr. 6, 62. https://doi.org/10.1525/elementa.316.

Boesch, D.F., Atkinson, L.P., Bolocourt, W.C., Boon, J.D., Cahoon, D.R., Dalrymple, R.A., Ezer, T., Horton, B.P., Johnson, Z.P., Kopp, R.E., Li, M., Moss, R.H., Parris, A., Sommerfield, C.K., 2013. Updating Maryland's sea-level rise projections. Cambridge, MD. Report at: ⟨http://www.umces.edu/sites/default/files/pdfs/SeaLevelRiseProjections.pdf⟩. (Accessed 2021).

Box, G., Cox, D., 1964. An analysis of transformations. J. R. Stat. Soc. B (Methodological) 26, 211–252.

Bradford, M.A., Keiser, A.D., Davies, C.A., Mersmann, C.A., Strickland, M.S., 2013. Empirical evidence that soil carbon formation from plant inputs is positively related to microbial growth. Biogeochem. Lett. 113, 271–281. https://doi-org.proxy-um.researchport.umd.edu/10.1007/s10533-012-9822-0.

Bridgham, S.D., Megonigal, J.P., Keller, J.K., Bliss, N.B., Trettin, C., 2006. The carbon balance of North American wetlands. Wetlands 26, 889–916.

Bronick, C.J., Lal, R., 2005. Soil structure and management: a review. Geoderma 124, 3–22. https://doi.org/10.1016/j.geoderma.2004.03.005.

Center for International Earth Science Information Network Socioeconomic Data and Applications Center (CIESEN SEDAC), 2020. Marine and Coastal Regions and Sea

Level Rise. ⟨https://sedac.ciesin.columbia.edu/theme/marine-and-coastal/maps/services⟩. (Accessed 2020).
Chambers, L.G., Osborne, T.Z., Reddy, K.R., 2013. Effect of salinity-altering pulsing events on soil organic carbon loss along an intertidal wetland gradient: a laboratory experiment. Biogeochemistry 115, 363–383. https://doi.org/10.1007/s10533-013-9841-5.
Chen, C.-C., McCarl, B., Chang, C.-C., 2012. Climate change, sea level rise and rice: global market implications. Clim. Chang. 110, 543–560. https://doi.org/10.1007/s10584-011-0074-0.
Chesapeake Bay Program, 2021. Chesapeake Bay Program: Water Quality Database. ⟨https://www.chesapeakebay.net/what/downloads/cbp_water_quality_database_1984_present⟩. (Accessed 2021).
Chmura, G.L., Anisfeld, S.C., Cahoon, D.R., Lynch, J.C., 2003. Global carbon sequestration in tidal, saline wetland soils. Glob. Biogeochem. Cycles 17, n/a. https://doi.org/10.1029/2002GB001917.
Church, J.A., Clark, P.U., Cazenave, A., Gregory, J.M., Jevrejeva, S., Levermann, A., Merrifield, M.A., Milne, G.A., Nerem, R.S., Nunn, P.D., Payne, A.J., Pfeffer, W.T., Stammer, D., Unnikrishnan, A.S., 2013. Sea level change. In: Climate Change 2013: The Physical Science Basis. Contribution of Working Group I to the Fifth Assessment Report of the Intergovernmental Panel on Climate Change. Cambridge University Press.
Cotrufo, M., Soong, J., Horton, A., Campbell, E., Haddix, M., Wall, D., Parton, W., 2015. Formation of soil organic matter via biochemical and physical pathways of litter mass loss. Nat. Geosci. 8, 776–779. https://doi.org/10.1038/ngeo2520.
Cotrufo, M.F., Wallenstein, M.D., Boot, C.M., Denef, K., Paul, E., 2013. The Microbial Efficiency-Matrix Stabilization (MEMS) framework integrates plant litter decomposition with soil organic matter stabilization: do labile plant inputs form stable soil organic matter? Glob. Chang. Biol. 19, 988–995. https://doi.org/10.1111/gcb.12113.
Drury, C.F., Stone, J.A., Findlay, W.I., 1991. Microbial biomass and soil structure associated with corn, grasses, and legumes. Soil Sci. Soc. Am. J. 55, 805–811. https://doi.org/10.2136/sssaj1991.03615995005500030029x.
Dungait, J.A.J., Hopkins, D.W., Gregory, A.S., Whitmore, A.P., 2012. Soil organic matter turnover is governed by accessibility not recalcitrance. Glob. Chang. Biol. 18, 1781–1796. https://doi.org/10.1111/j.1365-2486.2012.02665.x.
Ezer, T., Corlett, W.B., 2012. Is sea level rise accelerating in the Chesapeake Bay? A demonstration of a novel new approach for analyzing sea level data. Geophys. Res. Lett. 39 (19), 1–56. https://doi.org/10.1029/2012GL053435.
Fan, J., McConkey, B., Wang, H., Janzen, H., 2016. Root distribution by depth for temperate agricultural crops. Field Crop. Res. 189, 68–74. https://doi.org/10.1016/j.fcr.2016.02.013.
Feng, X., Simpson, M., 2007. The distribution and degradation of biomarkers in Alberta grassland soil profiles. Org. Geochem. 38, 1558–1570. https://doi.org/10.1016/j.orggeochem.2007.05.001.
Gedan, K.B., Fernández-Pascual, E., 2019. Salt marsh migration into salinized agricultural fields: a novel assembly of plant communities. J. Veg. Sci. 30, 1007–1016. https://doi.org/10.1111/jvs.12774.
Gedan, K.B., Epanchin-Niell, R., Qi, M., 2020. Rapid land cover change in a submerging coastal county. Wetlands 30, 1007–1016. https://doi.org/10.1007/s13157-020-01328-y.
Google Earth, 2020. Google Earth imagery. Google. ⟨http://www.earth.google.com⟩.
Gopalakrishnan, T., Hasan, M., Haque, A., Jayasinghe, S., Kumar, L., 2019. Sustainability of coastal agriculture under climate change. Sustainability 11, 7200. https://doi.org/10.3390/su11247200.
Grandy, A.S., Robertson, G.P., 2007. Land-use intensity effects on soil organic carbon accumulation rates and mechanisms. Ecosystems 10, 59–74. https://doi.org/10.1007/s10021-006-9010-y.
Hall, S.J., Berhe, A.A., Thompson, A., 2018. Order from disorder: do soil organic matter composition and turnover co-vary with iron phase crystallinity? Biogeochemistry 140, 93–110. https://doi.org/10.1007/s10533-018-0476-4.
Herbert, E.R., Schubauer-Berigan, J., Craft, C.B., 2018. Differential effects of chronic and acute simulated seawater intrusion on tidal freshwater marsh carbon cycling. Biogeochemistry 138, 137–154. https://doi.org/10.1007/s10533-018-0436-z.
Hothorn, T., Bretz, F., Westfall, P., 2008. Simultaneous inference in general parametric models. Biom. J. 50, 346–363. https://doi.org/10.1002/bimj.200810425.
Houghton, R.A., Hackler, J.L., 2008. Carbon Flux to the Atmosphere from Land-Use Changes 1850–1990. https://doi.org/10.3334/CDIAC/lue.ndp050.
Huggins, D.R., Reganold, J.P., 2008. No-till: the quiet revolution. Sci. Am. 299, 70–77. https://doi.org/10.1038/scientificamerican0708-70.
Jastrow, J.D., Amonette, J.E., Bailey, V.L., 2007. Mechanisms controlling soil carbon turnover and their potential application for enhancing carbon sequestration. Clim. Chang. 80, 5–23. https://doi.org/10.1007/s10584-006-9178-3.
Jones, D., Nguyen, C., Finlay, R., 2009. Carbon flow in the rhizosphere: carbon trading at the soil–root interface. Plant Soil 321, 5–33. https://doi.org/10.1007/s11104-009-9925-0.
Kell, D.B., 2012. Large-scale sequestration of atmospheric carbon via plant roots in natural and agricultural ecosystems: why and how. Philos. Trans. R. Soc. B Biol. Sci. 367, 1589–1597. https://doi.org/10.1098/rstb.2011.0244.
Lehmann, J., Kleber, M., 2015. The contentious nature of soil organic matter. Nature 528, 60–68. https://doi.org/10.1038/nature16069.
Lorenz, K., Lal, R., 2005. The depth distribution of soil organic carbon in relation to land use and management and the potential of carbon sequestration in subsoil horizons. Adv. Agron. 88, 35–66. https://doi.org/10.1016/S0065-2113(05)88002-2.
von Lützow, M., Kögel-Knabner, I., Ekschmitt, K., Matzner, E., Guggenberger, G., Marschner, B., Flessa, H., 2006. Stabilization of organic matter in temperate soils: mechanisms and their relevance under different soil conditions - a review. Eur. J. Soil Sci. 57, 426–445. https://doi.org/10.1111/j.1365-2389.2006.00809.x.
von Lützow, M., Kögel-Knabner, I., Ekschmitt, K., Flessa, H., Guggenberger, G., Matzner, E., Marschner, B., 2007. SOM fractionation methods: relevance to functional pools and to stabilization mechanisms. Soil Biol. Biochem. 39, 2183–2207. https://doi.org/10.1016/j.soilbio.2007.03.007.
Martens, D.A., Reedy, T.E., Lewis, D.T., 2004. Soil organic carbon content and composition of 130-year crop, pasture and forest land-use managements. Glob. Chang. Biol. 10, 65–78. https://doi.org/10.1046/j.1529-8817.2003.00722.x.
Maryland Department of Planning (MDP), 2019. State of Maryland Plan to Adapt to Saltwater Intrusion and Salinization. Dubow, J., Cornwell, D.H. (primary authors). Andreasen, D., Staley, A., Tully, K., Gedan, K., Epanchin-Niell, R (contributing authors). ⟨https://planning.maryland.gov/Documents/OurWork/envr-planning/2019–1212-Marylands-plan-to-adapt-to-saltwater-intrusion-and-salinization.pdf⟩. (Accessed 2020).
Mcleod, E., Chmura, G.L., Bouillon, S., Salm, R., Björk, M., Duarte, C.M., Lovelock, C.E., Schlesinger, W.H., Silliman, B.R., 2011. A blueprint for blue carbon: toward an improved understanding of the role of vegetated coastal habitats in sequestering CO_2. Front. Ecol. Environ. 9, 552–560. https://doi.org/10.1890/110004.
Mitsch, W.J., Gosselink, J.G., 2015. Wetlands, fifth ed. John Wiley & Sons, Inc., Hoboken, NJ, USA.
Morris, J.T., Barber, D.C., Callaway, J.C., Chambers, R., Hagen, S.C., Hopkinson, C.S., Johnson, B.J., Megonigal, P., Neubauer, S.C., Troxler, T., Wigand, C., 2016. Contributions of organic and inorganic matter to sediment volume and accretion in tidal wetlands at steady state: SEDIMENT BULK DENSITY AND IGNITION LOSS. Earths Future 4, 110–121. https://doi.org/10.1002/2015EF000334.
Paul, E.A., Kravchenko, A., Grandy, A.S., Morris, S., 2015. Soil Organic Matter Dynamics: controls and management for sustainable ecosystem functioning. In: The Ecology of Agricultural Landscapes: Long-Term Research on the Path to Sustainability. Oxford University Press, New York, New York, USA, pp. 104–134.
Perfect, E., Kay, B.D., van Loon, W.K.P., Sheard, R.W., Pojasok, T., 1990. Factors influencing soil structural stability within a growing season. Soil Sci. Soc. Am. J. 54, 173–179. https://doi.org/10.2136/sssaj1990.03615995005400010027x.
Poirier, V., Roumet, C., Munson, A.D., 2018. The root of the matter: linking root traits and soil organic matter stabilization processes. Soil Biol. Biochem. 120, 246–259. https://doi.org/10.1016/j.soilbio.2018.02.016.
R Core Team, 2019. R: a language and environment for statistical computing. R Foundation for Statistical Computing, Vienna, Austria. ⟨https://www.R-project.org/⟩.
Rabenhorst, M.C., 2008. Protocol for Using and Interpreting IRIS Tubes. Soil Surv. Horiz. 49, 74–77. https://doi.org/10.2136/sh2008.3.0074.
Sanaullah, M., Chabbi, A., Leifeld, J., Bardoux, G., Billou, D., Rumpel, C., 2010. Decomposition and stabilization of root litter in top- and subsoil horizons: what is the difference? Plant Soil 338, 127–141. https://doi.org/10.1007/s11104-010-0554-4.
Sarkar, B., Singh, M., Mandal, S., Churchman, G.J., Bolan, N.S., 2018. Clay minerals—organic matter interactions in relation to carbon stabilization in soils. In: The Future of Soil Carbon. Elsevier, pp. 71–86. https://doi.org/10.1016/B978-0-12-811687-6.00003-1.
Schmidt, M.W.I., Torn, M.S., Abiven, S., Dittmar, T., Guggenberger, G., Janssens, I.A., Kleber, M., Kögel-Knabner, I., Lehmann, J., Manning, D.A.C., Nannipieri, P., Rasse, D.P., Weiner, S., Trumbore, S.E., 2011. Persistence of soil organic matter as an ecosystem property. Nature 478, 49–56. https://doi.org/10.1038/nature10386.
Singer, M.J., Southard, R.J., Warrington, D.N., Janitzky, P., 1992. Stability of synthetic sand-clay aggregates after wetting and drying cycles. Soil Sci. Soc. Am. J. 56, 1843–1848. https://doi.org/10.2136/sssaj1992.03615995005600060032x.
Six, J., Paustian, K., Elliott, E.T., Combrink, C., 2000. Soil structure and organic matter I. Distribution of aggregate-size classes and aggregate-associated carbon. Soil Sci. Soc. Am. J. 64, 681–689.
Sollins, P., Homann, P., Caldwell, B.A., 1996. Stabilization and destabilization of soil organic matter: mechanisms and controls. Geoderma 74, 65–105. https://doi.org/10.1016/S0016-7061(96)00036-5.
Stockmann, U., Adams, M.A., Crawford, J.W., Field, D.J., Henakaarchchi, N., Jenkins, M., Minasny, B., McBratney, A.B., Courcelles, V., de, R., de, Singh, K., Wheeler, I., Abbott, L., Angers, D.A., Baldock, J., Bird, M., Brookes, P.C., Chenu, C., Jastrow, J.D., Lal, R., Lehmann, J., O'Donnell, A.G., Parton, W.J., Whitehead, D., Zimmermann, M., 2013. The knowns, known unknowns and unknowns of sequestration of soil organic carbon. Agric. Ecosyst. Environ. 164, 80–99. https://doi.org/10.1016/j.agee.2012.10.001.
Syswerda, S.P., Corbin, A.T., Mokma, D.L., Kravchenko, A.N., Robertson, G.P., 2011. Agricultural management and soil carbon storage in surface vs. deep layers. Soil Sci. Soc. Am. J. 75, 92–101. https://doi.org/10.2136/sssaj2009.0414.
Thanh, N.C., 2016. Saltwater intrusion - an evident impact of climate change in the MD and propose adaptable solutions. Am. J. Environ. Resour. Econ. 1, 1–8. https://doi.org/10.11648/j.ajere.20160101.11.
Tisdall, J.M., Oades, J.M., 1982. Organic matter and water-stable aggregates in soils. J. Soil Sci. 33, 141–163. https://doi.org/10.1111/j.1365-2389.1982.tb01755.x.
Tully, K.L., Gedan, K., Epanchin-Niell, R., Strong, A., Bernhardt, E.S., BenDor, T., Mitchell, M., Kominoski, J., Jordan, T.E., Neubauer, S.C., Weston, N.B., 2019a. The invisible flood: the chemistry, ecology, and social implications of coastal saltwater intrusion. BioScience 69, 368–378. https://doi.org/10.1093/biosci/biz027.
Tully, K.L., Weissman, D., Wyner, W.J., Miller, J., Jordan, T., 2019b. Soils in transition: saltwater intrusion alters soil chemistry in agricultural fields. Biogeochemistry 142, 339–356. https://doi.org/10.1007/s10533-019-00538-9.

U.S. Department of Agriculture Natural Resources Conservation Service (USDANRCS), 2017. The PLANTS Database. ⟨https://plants.sc.egov.usda.gov/java/⟩. (Accessed 2020).
U.S. Department of Agriculture Natural Resources Conservation Service (USDANRCS), 2020. Web Soil Survey. ⟨https://websoilsurvey.sc.egov.usda.gov/⟩. (Accessed 2020).
Wahid, P.A., Kamalam, N.V., 1993. Reductive dissolution of crystalline and amorphous Fe (III) oxides by microorganisms in submerged soil. Biol. Fertil. Soils 15, 144–148.
Watteau, F., Villemin, G., Burtin, G., Jocteur-Monrozier, L., 2006. Root impact on the stability and types of micro-aggregates in silty soil under maize. Eur. J. Soil Sci. 57 (2), 247–257. https://doi.org/10.1111/j.1365-2389.2005.00734.x.
Weil, R.R., Brady, N.C., 2016. The Nature and Properties of Soil, 15th ed. Pearson, Columbus, OH.
Weston, N.B., Dixon, R.E., Joye, S.B., 2006. Ramifications of increased salinity in tidal freshwater sediments: geochemistry and microbial pathways of organic matter mineralization. J. Geophys. Res. 111 https://doi.org/10.1029/2005JG000071.
Weston, N.B., Vile, M.A., Neubauer, S.C., Velinsky, D.J., 2011. Accelerated microbial organic matter mineralization following salt-water intrusion into tidal freshwater marsh soils. Biogeochemistry 102, 135–151. https://doi.org/10.1007/s10533-010-9427-4.
Wichelns, D., Qadir, M., 2015. Achieving sustainable irrigation requires effective management of salts, soil salinity, and shallow groundwater. Agric. Water Manag. 157, 31–38. https://doi.org/10.1016/j.agwat.2014.08.016.
Wilson, M.J., 1999. The origin and formation of clay minerals in soils: past, present and future perspectives. Clay Miner. 34, 7–25. https://doi.org/10.1180/000985599545957.